Electronic Supplementary Information

Foldamer-based Helicate Displaying Reversible Switching between Two Distinct Conformers

Hae-Geun Jeon, Hyun Kyung Lee, Seungwon Lee and Kyu-Sung Jeong*

**Department of Chemistry, Yonsei University, Seoul 03722, Korea*

Fax: +82-2-364-7050

Tel: +82-2123-2643

E-mail: ksjeong@yonsei.ac.kr;

Contents

1. Syntheses and characterisation of new compounds

1.1 General: All chemicals were purchased from commercial suppliers and used without further purification unless otherwise specified. Dichloromethane (CH_2Cl_2) was purified by drying over calcium hydride (CaH_2), followed by distillation. Hexane and ethyl acetate (EtOAc) were distilled. Water-saturated deuterated solvents were prepared by sonicating the organic solvent containing a few drops of distilled water for 10 min. After 1 h standing, organic layer was carefully separated out for use. Thin layer chromatography (TLC) was performed on Merck (silica gel 60, F-254, 0.25 mm). Silica gel 60 (230-400 mesh, Merck) was used for column chromatography. Melting points were determined with a Barnstead Electrothermal (IA9100) apparatus. FT-IR spectra were measured by using a Vertex70 FT-IR spectrometer. 1D and 2D NMR spectra were measured by using Bruker Avance II DRX 400 and Avance III HD 300 instruments. Chemical shifts were reported using residual protonated solvent peaks (for ^{1}H NMR spectra, acetone-d_6 2.05 ppm; CD_2Cl_2 5.32 ppm; $(CD_2Cl)_2$ 3.72 ppm; DMSO-d_6 2.50 ppm; dioxane-d_8 3.53 ppm; toluene-d_8 7.09 ppm; and for ^{13}C NMR spectra, acetone-d_6 206.26 ppm; CD_2Cl_2 53.84 ppm; DMSO-d_6 39.52 ppm), and tetramethylsilane (TMS) peak as an internal standard for ethyl acetate-d_8. The ESI-HRMS spectrometric measurements were obtained from *the Organic Chemistry Research Center* at Sogang University.

General procedure of Sonogashira coupling reaction: A Schlenk flask containing two coupling compounds, CuI and $Pd(PPh_3)_2Cl_2$ was evacuated under vacuum and back-filled with nitrogen. Anhydrous, degassed tetrahydrofuran (THF) and triethylamine (Et_3N) were added sequentially and the solution was stirred under the given conditions. The mixture was filtered through Celite and concentrated, and the residue was dissolved in CH_2Cl_2. The solution was washed with $NaHCO_3$ and brine, dried over anhydrous Na_2SO_4 and concentrated. The residue was purified by flash column chromatography (silica gel).

1.2 Synthesis of compound 1

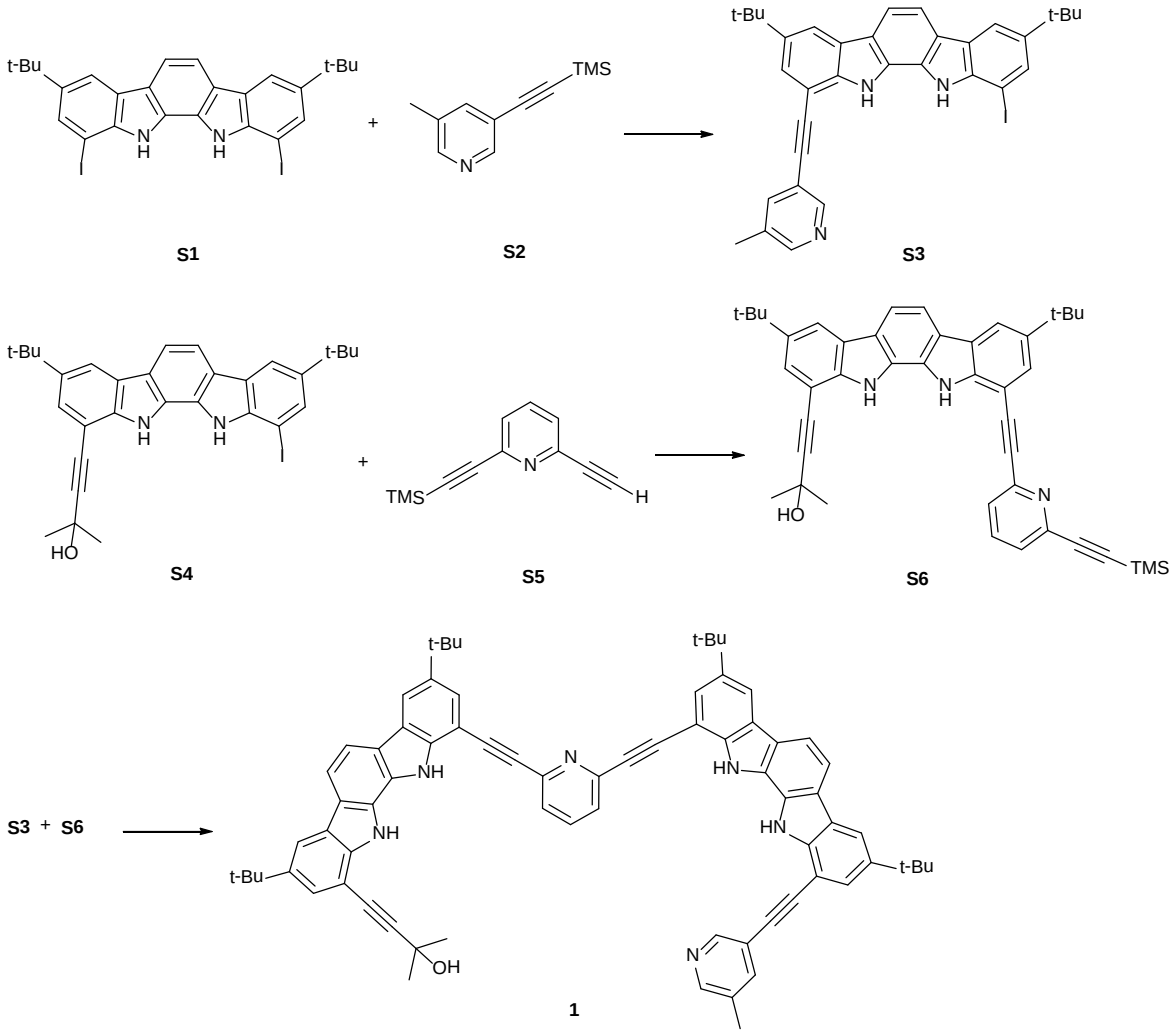

S3: Compound **S3** was synthesised according to the general procedure using **S1**[S1] (322 mg, 0.52 mmol), **S2**[S2] (33 mg, 0.17 mmol), CuI (2.5 mg, 0.013 mmol), $Pd(PPh_3)_2Cl_2$ (6.0 mg, 0.009 mmol), THF (1.5 mL) and Et_3N (1.0 mL). Reaction time 4.5 h; eluent: EtOAc/*n*-hexane = 1:2 (v/v); green solid; 83% yield (88 mg); mp > 235 ºC (dec); ^{1}H NMR (400 MHz, acetone-d_6, 25 °C) δ ppm 10.63 (s, 1H, NH), 9.91 (s, 1H, NH), 8.68 (s, 1H), 8.50 (s, 1H), 8.37 (s, 1H), 8.29 (s, 1H), 8.07 (d, *J* = 8.29, 1H), 8.02 (d, *J* = 8.36, 1H), 7.88 (s, 2H), 7.73 (s, 1H), 2.44 (s, 3H), 1.50 (s, 9H, *t*-Bu), 1.47 (s, 9H, *t*-Bu) ^{13}C NMR (100 MHz, acetone-d_6, 25 °C) δ ppm 150.4, 150.0, 145.6, 143.5, 140.4, 139.3, 139.2, 134.0, 132.2, 127.0, 126.7, 126.6, 125.4, 125.2, 123.1, 122.5, 120.6, 118.7, 117.3, 113.5, 105.5, 90.7, 89.9, 76.4, 35.3, 35.3, 32.2, 18.2;

[S1] (*a*) K.-J. Chang, D. Moon, M. S. Lah and K.-S. Jeong, *Angew. Chem. Int. Ed.*, 2005, **44**, 7926; (*b*) N.-K. Kim, K.-J. Chang, D. Moon, M. S. Lah and K.-S. Jeong, *Chem. Commun.*, 2007, 3401.
[S2] B. Song, Z. Zhang, K. Wang, C.-H. Hsu, O. Bolarinwa, J. Wang, Y. Li, G.-Q. Yin, E. Rivera, H.-B. Yang, C. Liu, B. Xu and X. Li, *Angew. Chem. Int. Ed.*, 2017, **56**, 5258.

MALDI-TOF *m/z* calcd for $C_{34}H_{32}IN_3$ 609, found 610; ESI-HRMS *m/z* calcd for $C_{34}H_{33}IN_3$ $[M+H]^+$ 610.1719, found $[M+H]^+$ 610.1717; IR (KBr) υ 3585 (O–H), 3413 (N–H), 2208 (C≡C) cm^{-1}.

S6: Compound **S6** was synthesised according to the general procedure using **S4**[S3] (420 mg, 0.729 mmol), **S5**[S4] (176 mg, 0.883 mmol), CuI (5.0 mg, 0.026 mmol), $Pd(PPh_3)_2Cl_2$ (12 mg, 0.017 mmol), THF (4.2 mL) and Et_3N (3.5 mL). Reaction time 3 h; eluent: diethyl ether/*n*-hexane = 1:2 (v/v); yellow solid; 89% yield (422 mg); mp > 227 ºC (dec); ^{1}H NMR (400 MHz, DMSO-d_6, 25 °C) δ ppm 11.38 (s, 1H, NH), 10.95 (s, 1H, NH), 8.35 (s, 1H), 8.23 (s, 1H), 8.03 (s, 2H), 7.96 (t, *J* = 7.75, 1H), 7.84 (d, *J* = 7.53, 1H), 7.74 (s, 1H), 7.61 (d, *J* = 7.33, 1H), 7.48 (s, 1H), 5.65 (s, 1H, OH), 1.65 (s, 6H, Me), 1.46 (s, 9H, *t*-Bu), 1.42 (s, 9H, *t*-Bu), 0.29 (s, 9H); ^{13}C NMR (100 MHz, DMSO-d_6, 25 °C) δ ppm 143.0, 142.4, 142.1, 141.9, 137.8, 137.6, 137.3, 127.4, 126.8, 126.3, 126.0, 125.8, 125.6, 124.1, 123.7, 120.8, 120.5, 118.6, 116.9, 112.3, 112.2, 104.9, 103.5, 103.0, 99.7, 94.8, 91.8, 86.9, 77.5, 64.0, 34.5, 34.4, 31.9, 31.7, −0.41; MALDI-TOF *m/z* calcd for $C_{43}H_{45}N_3OSi$ 647, found 648; ESI-HRMS *m/z* calcd for $C_{43}H_{46}N_3OSi$ $[M+H]^+$ 648.3410, found $[M+H]^+$ 648.3407; IR (KBr) υ 3420 (N–H), 2207 (C≡C), 1279 (Si–CH_3), 1127 (C–O) cm^{-1}.

1: A Schlenk flask containing **S6** (120 mg, 0.185 mmol), **S3** (115 mg, 0.189 mmol), CuI (2.0 mg, 0.011 mmol) and $Pd(PPh_3)_2Cl_2$ (5.0 mg, 0.007 mmol) was evacuated under vacuum and back-filled with nitrogen. Anhydrous, degassed THF (1.1 mL), Et_3N (1.0 mL) and *n*-tetrabutylammonium fluoride (0.23 mL, 1.0 M solution in THF) were added in order and the solution was stirred at room temperature for 3 hours. The mixture was filtered through Celite and concentrated. The residue was dissolved in CH_2Cl_2, washed with water and brine, and dried over anhydrous Na_2SO_4. After concentration under reduced pressure, the residue was purified by flash column chromatography (silica gel, EtOAc/*n*-hexane = 2:3 (v/v)) to give **1** (178 mg, 91%) as a yellow solid; mp > 212 ºC (dec); ^{1}H NMR (400 MHz, DMSO-d_6, 25 °C) δ ppm 11.40 (s, 1H, NH), 11.20 (s, 2H, NH), 10.89 (s, 1H, NH), 8.68 (s, 1H), 8.39 (s, 2H), 8.33 (s, 1H), 8.22 (s, 1H), 8.17 (s, 1H), 8.08 (m, 5H), 7.95 (d, 2H), 7.90 (s, 1H), 7.76 (s, 1H),

[S3] J. I. Kim, H. Juwarker, X. Liu, M. S. Lah and K.-S. Jeong, *Chem. Commun.*, 2010, **46**, 764.
[S4] A. Orita, T. Nakano, D. L. An, K. Tanikawa, K. Wakamatsu and J. Otera, *J. Am. Chem. Soc*., 2004, **126**, 10389.

7.73 (s, 1H), 7.66 (s, 1H), 7.45 (s, 1H), 5.53 (s, 1H, OH), 2.12 (s, 3H, Me), 1.50 (s, 6H, Me), 1.49 (s, 9H, *t*-Bu), 1.46 (s, 9H, *t*-Bu), 1.44 (s, 9H, *t*-Bu), 1.41 (s, 9H, *t*-Bu); ^{13}C NMR (100 MHz, DMSO-d_6, 25 °C) δ ppm 149.4, 148.8, 143.2, 143.2, 142.2,142.1, 142.1, 141.8,138.6, 137.9, 137.7, 137.7, 137.7, 137.3, 132.9, 127.3, 126.1, 126.0, 126.0, 125.8, 125.8, 125.6, 125.4, 124.1, 124.1, 123.8, 123.8, 123.7, 120.8, 120.8, 120.6, 120.5, 119.0, 118.6,118.6, 118.0, 116.8,112.5, 112.4, 112.4, 112.2,104.8, 103.9, 103.1, 103.0, 99.7, 91.9, 91.8, 89.8, 89.2, 87.1, 86.9, 77.4, 63.9, 34.6, 34.6, 34.6, 34.4, 32.7, 32.7, 32.7, 32.7, 32.7, 32.7, 32.7, 32.7, 32.7, 32.7, 32.7, 32.7, 32.7, 17.3; ESI-HRMS *m/z* calcd for $C_{74}H_{70}N_6O$ $[M+H]^+$ 1057.5533, found $[M+H]^+$ 1057.5533; IR (KBr) υ 3401 (N–H), 2205 (C≡C), 1159 (C–O) cm^{-1}.

1.3 Synthesis of compound 2

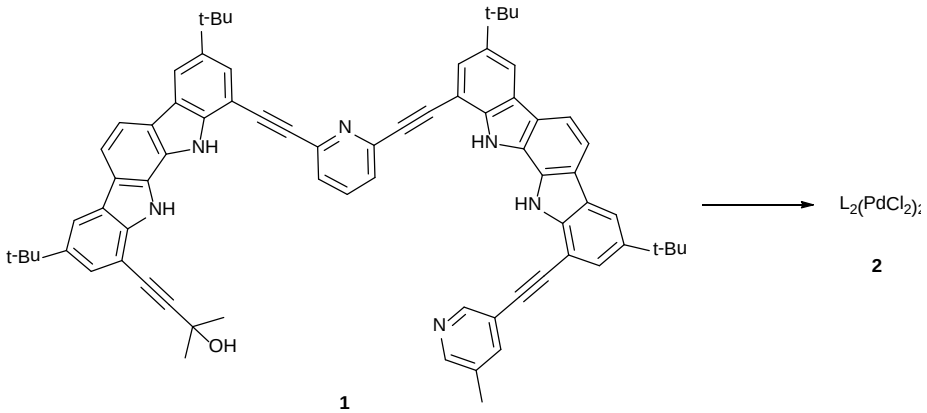

2: Ligand (**1**) (620 mg, 0.586 mmol) was dissolved in 1,2-dichloroethane (147 mL) and $Pd(CH_3CN)_2Cl_2$ solution (29.3 mL, 10 mM in acetone) were slowly added to the solution. The mixture were heated at 60 °C for 6 days and then cooled to ambient temperature. The residue was filtered off with a small amount of silica. The product was recrystallised from EtOAc/pentane, filtered, washed with pentane to give **2** (97 mg, 27%) as an orange solid; mp > 253 ºC (dec); ^{1}H NMR (400 MHz, CD_2Cl_2, 25 °C) δ ppm 11.10 (s, 1H, NH), 9.81 (s, 1H, NH), 9.32 (s, 1H, CH), 9.27 (s, 1H, NH), 9.22 (s, 1H, NH), 8.46 (s, 1H), 8.25 (s, 1H), 8.17 (s, 1H), 8.02 (m, 5H), 7.69 (d, *J* = 8.46 Hz, 1H), 7.64 (d, *J* = 8.05 Hz, 1H), 7.56 (s, 1H), 7.51 (d, *J* = 7.43 Hz, 1H), 7.41 (s, 1H), 7.36 (s, 1H), 7.34 (s, 1H), 7.15 (d, *J* = 8.17 Hz, 1H), 6.53 (s, 1H), 5.20 (s, 1H, OH), 1.89 (s, 3H, Me), 1.62 (s, 9H, *t*-Bu), 1.54 (s, 9H, *t*-Bu), 1.44 (s, 9H, *t*-Bu), 0.85 (s, 9H, *t*-Bu), 0.80 (s, 3H, Me); ^{13}C NMR (100 MHz, CD_2Cl_2, 25 °C) δ ppm 153.8, 150.4, 146.4, 145.2, 143.9, 143.2, 143.1, 142.9, 141.2, 139.4, 139.3, 139.0, 138.6, 137.5,

137.2, 128.6, 127.2, 126.5, 126.1, 125.9, 125.8, 125.6, 124.9, 124.6, 124.5, 122.9, 122.6, 121.9, 121.7, 121.4, 121.3, 120.6, 120.4, 118.7, 117.3, 113.2, 112.8, 112.4, 105.0, 104.2, 103.3, 101.4, 98.4, 97.8, 96.0, 94.1, 91.9, 91.0, 89.7, 79.8, 68.5, 35.4, 35.1, 35.1, 34.6, 34.0, 32.2, 32.2, 32.2, 32.1, 32.1, 32.1, 32.1, 32.1, 32.1, 31.2, 31.2, 31.2, 28.6, 16.8; ESI-HRMS *m/z* calcd for $C_{148}H_{136}Cl_4N_{12}O_2Pd_2$ $[M]^+$ 2468.7757, found $[M]^+$ 2468.7794; IR (KBr) υ 3352 (N–H), 2199 (C≡C), 1132 (C–O) cm^{-1}.

2. NMR studies

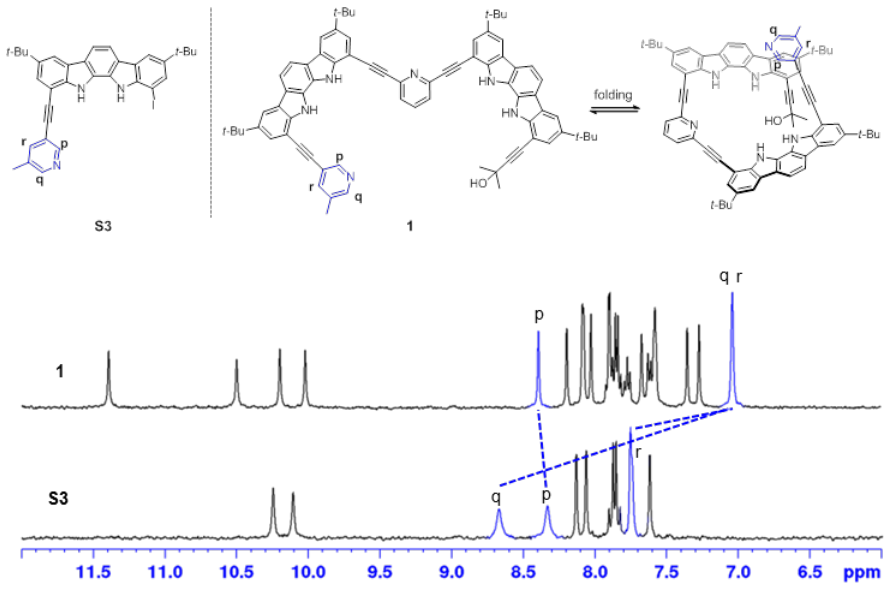

Fig. S1 Partial ^{1}H NMR spectra (300 MHz, 25 °C) of **S3** and **1** (1.0 mM in 1% (v/v) CD_3OH/water-saturated CD_2Cl_2). The blue-coloured peaks correspond to CH signals of terminal pyridine.

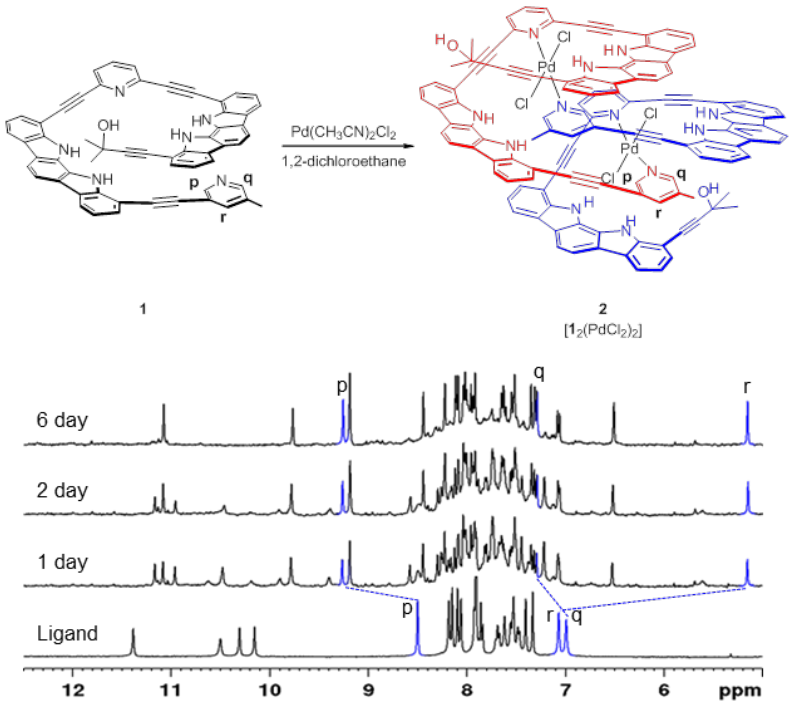

Fig. S2 Partial ^{1}H NMR spectra (400 MHz) of **1** during complex formation with $Pd(CH_3CN)_2Cl_2$ in 1,2-dichloroethane-d_4 at 60 °C.

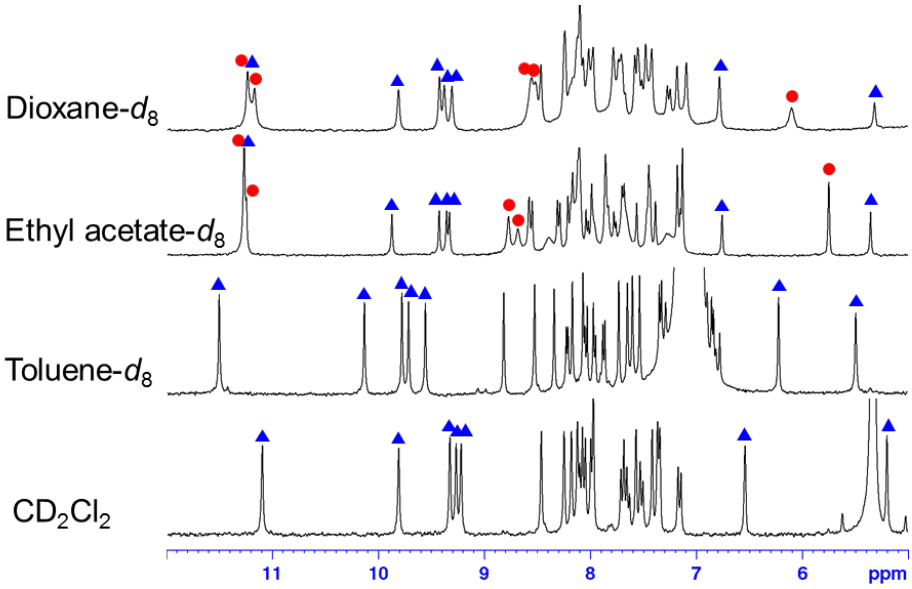

Fig. S3 Partial ^{1}H NMR spectra (300 MHz, 25 °C) of **2** (1.0 mM) in various solvents. Signals corresponding to **2**(*syn-anti*) and **2**(*syn-syn*) were marked by blue triangles and red circles, respectively.

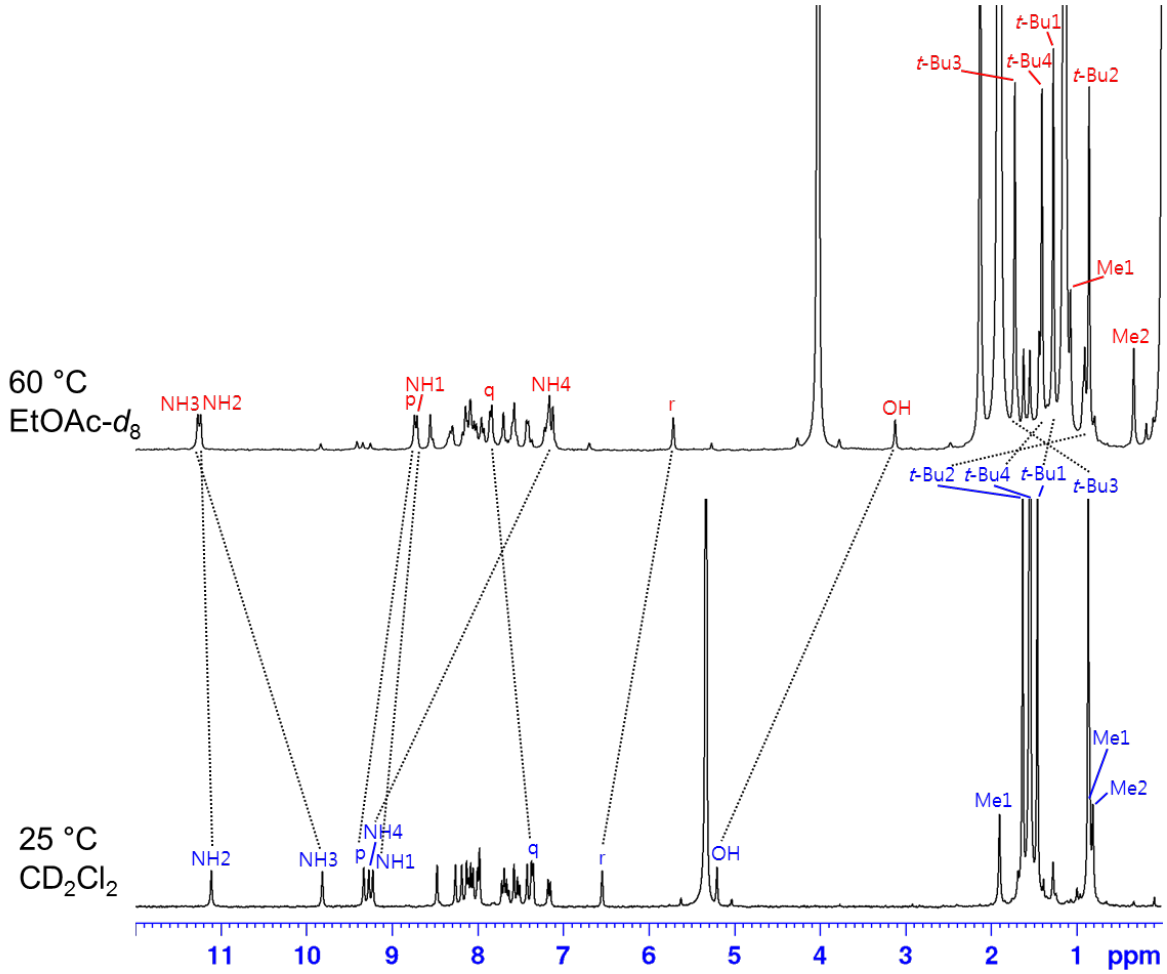

Fig. S4 ^{1}H NMR spectra (300 MHz) of **2** (1.0 mM) in CD_2Cl_2 at 25 °C (lower) and in ethyl acetate-d_8 at 60 °C (upper).

Table S1. ^{1}H NMR chemical shifts (ppm) of **2** (4.0 mM) in CD_2Cl_2 (25 °C, *syn-anti* conformation) and ethyl acetate-d_8 (60 °C, *syn-syn* conformation) and their differences.

		2 (*syn-anti*) (δ in CD_2Cl_2, 25 °C)	**2** (*syn-syn*) (δ in ethyl acetate-d_8, 60 °C)	difference (δ(CD_2Cl_2)-δ(ethyl acetate-d_8))
OH		5.19	3.13	2.06
NH	1	9.22	8.71	0.51
	2	11.1	11.23	−0.13
	3	9.81	11.27	−1.46
	4	9.27	7.16	2.11
t-Bu	1	1.45	1.28	0.17
	2	1.62	0.86	0.76
	3	0.85	1.73	−0.88
	4	1.54	1.41	0.13

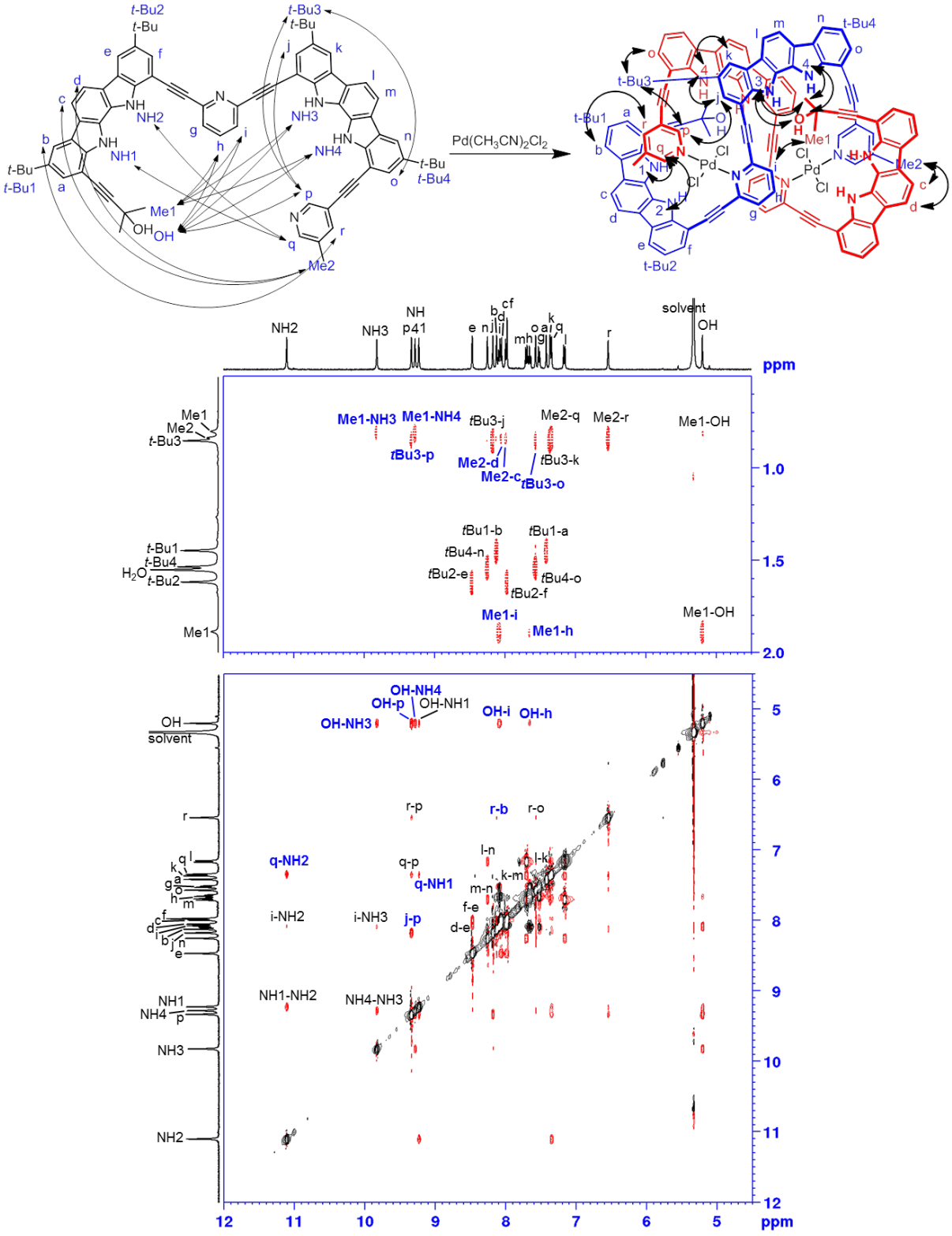

Fig. S5 Partial ROESY spectrum (CD_2Cl_2, 25 °C, mixing time: 400 ms) of **2** (2.0 mM).

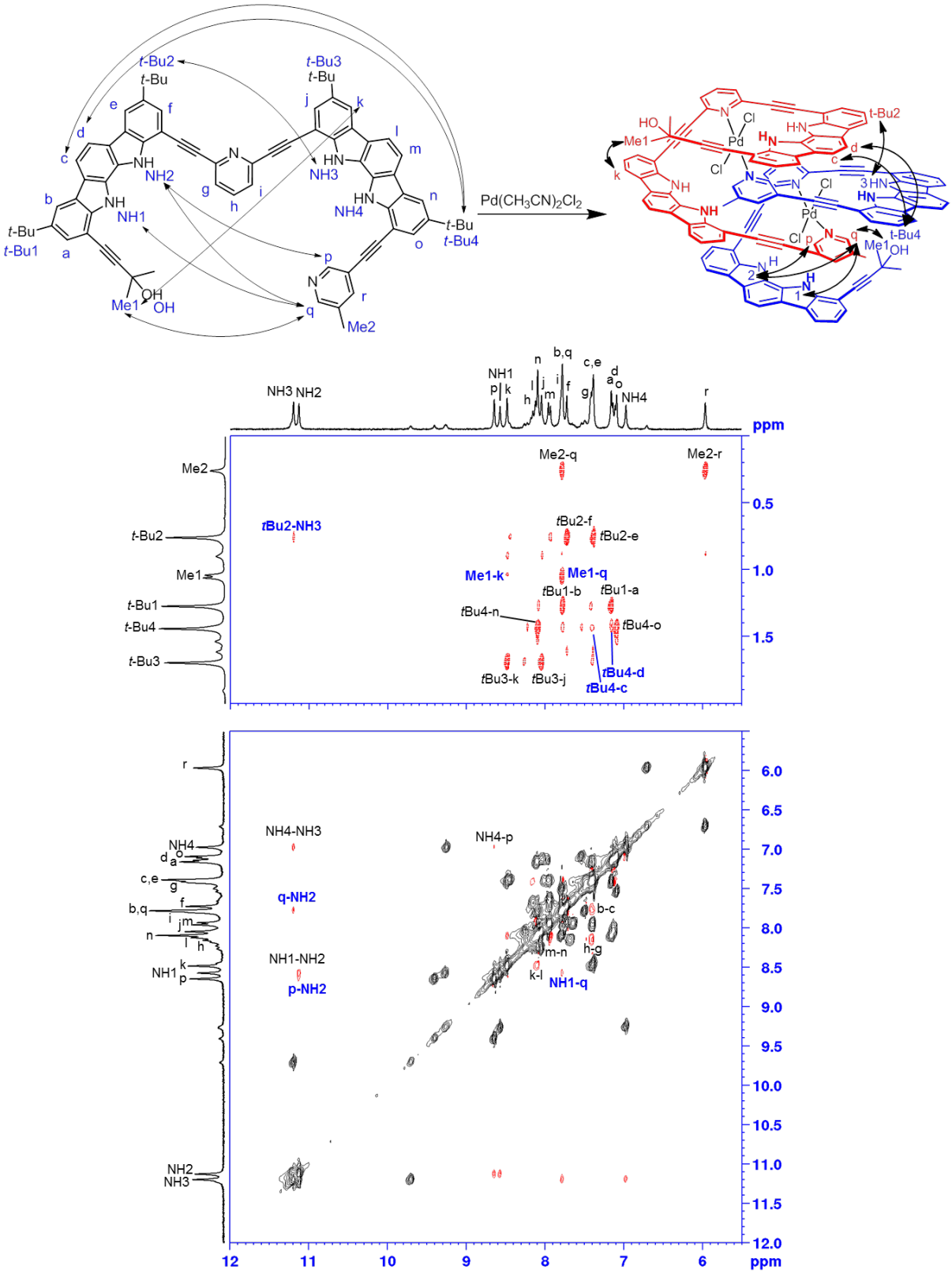

Fig. S6 Partial ROESY spectrum (dioxane-d_8, 80 °C, mixing time: 150 ms) of **2** (4.0 mM).

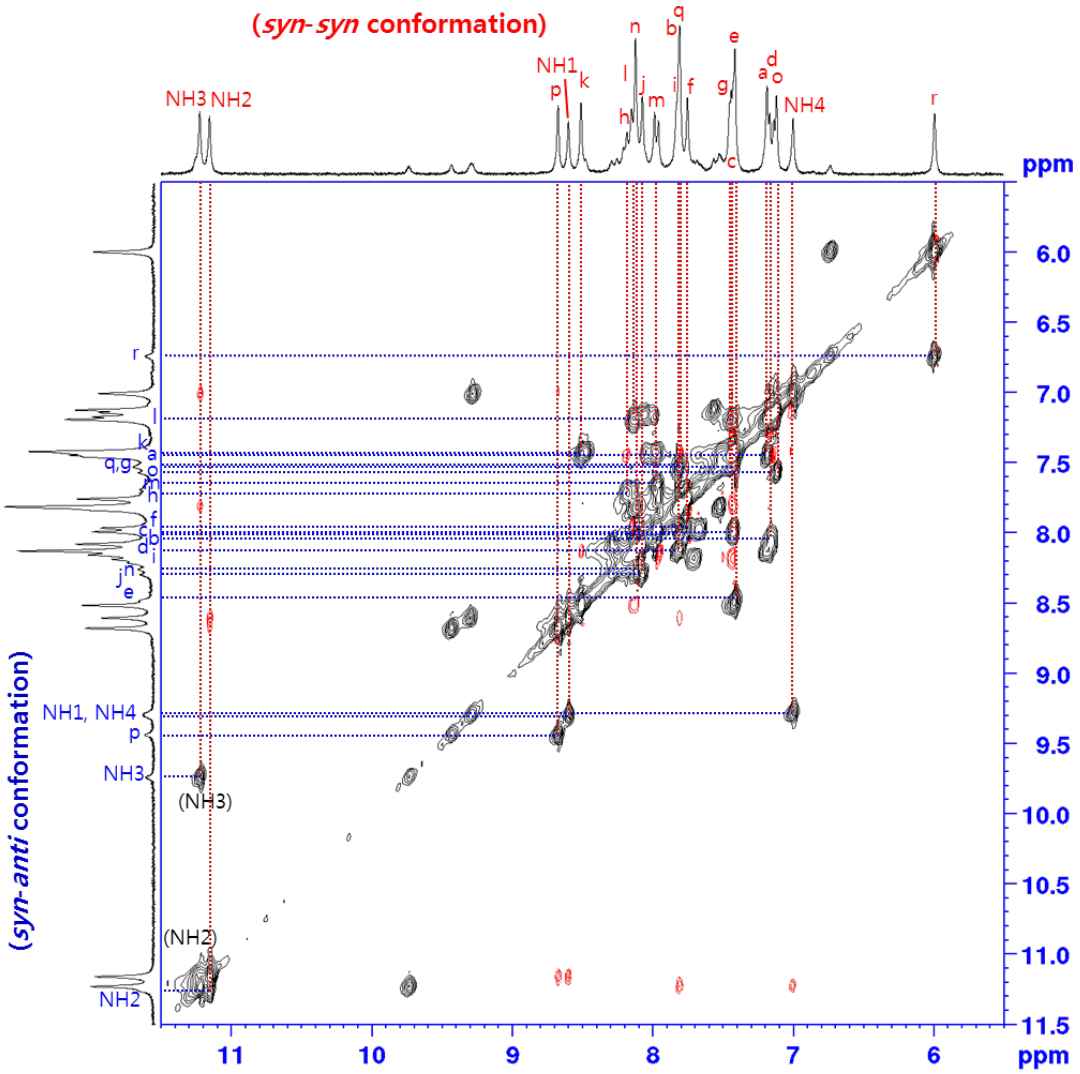

Fig. S7 Partial EXSY spectrum (dioxane-d_8, 80 °C, mixing time: 150 ms) of **2** (4.0 mM).

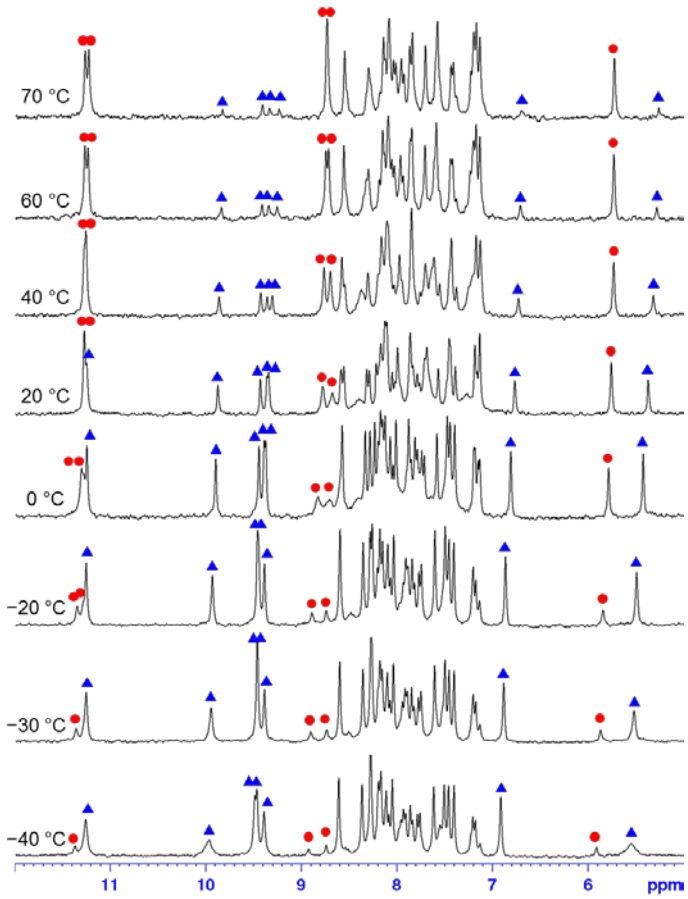

Fig. S8 Partial ^{1}H NMR spectra (300 MHz) of **2** (1.0 mM) in ethyl acetate-d_8 at various temperatures. Signals corresponding to **2**(*syn-anti*) and **2**(*syn-syn*) were marked by blue triangles and red circles, respectively.

Table S2. Relative populations of **2**(*syn-anti*) and **2**(*syn-syn*), determined by the integrations of ^{1}H NMR spectra at various temperatures in ethyl acetate-d_8.

Temperature (°C)	$I_{\mathbf{2}(syn\text{-}anti)}$	$I_{\mathbf{2}(syn\text{-}syn)}$
70	1	7.6493
60	1	6.5592
40	1	3.8506
25	1	2.1378
20	1	1.8083
0	1	0.806
−20	1	0.2897
−30	1	0.2302
−40	1	0.1176

$$K_{eq} = \frac{I_{\mathbf{2}(syn-syn)}}{I_{\mathbf{2}(syn-anti)}} \quad (1)$$

$$\ln(K_{eq}) = -\frac{\Delta H}{RT} + \frac{\Delta S}{R} \quad (2)$$

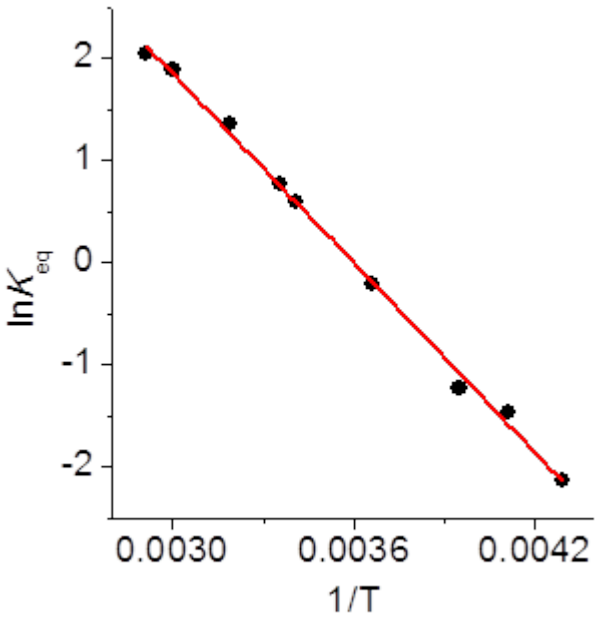

Fig. S9 A van't Hoff plot for the equilibriums of **2**(*syn-anti*) and **2**(*syn-syn*) between −40 and 70 °C in ethyl acetate-d_8. Δ*H*° and Δ*S*° were calculated employing equations (1) and (2) to be +26 kJ·mol^{-1} and +92 J·K^{-1}·mol^{-1}, respectively.

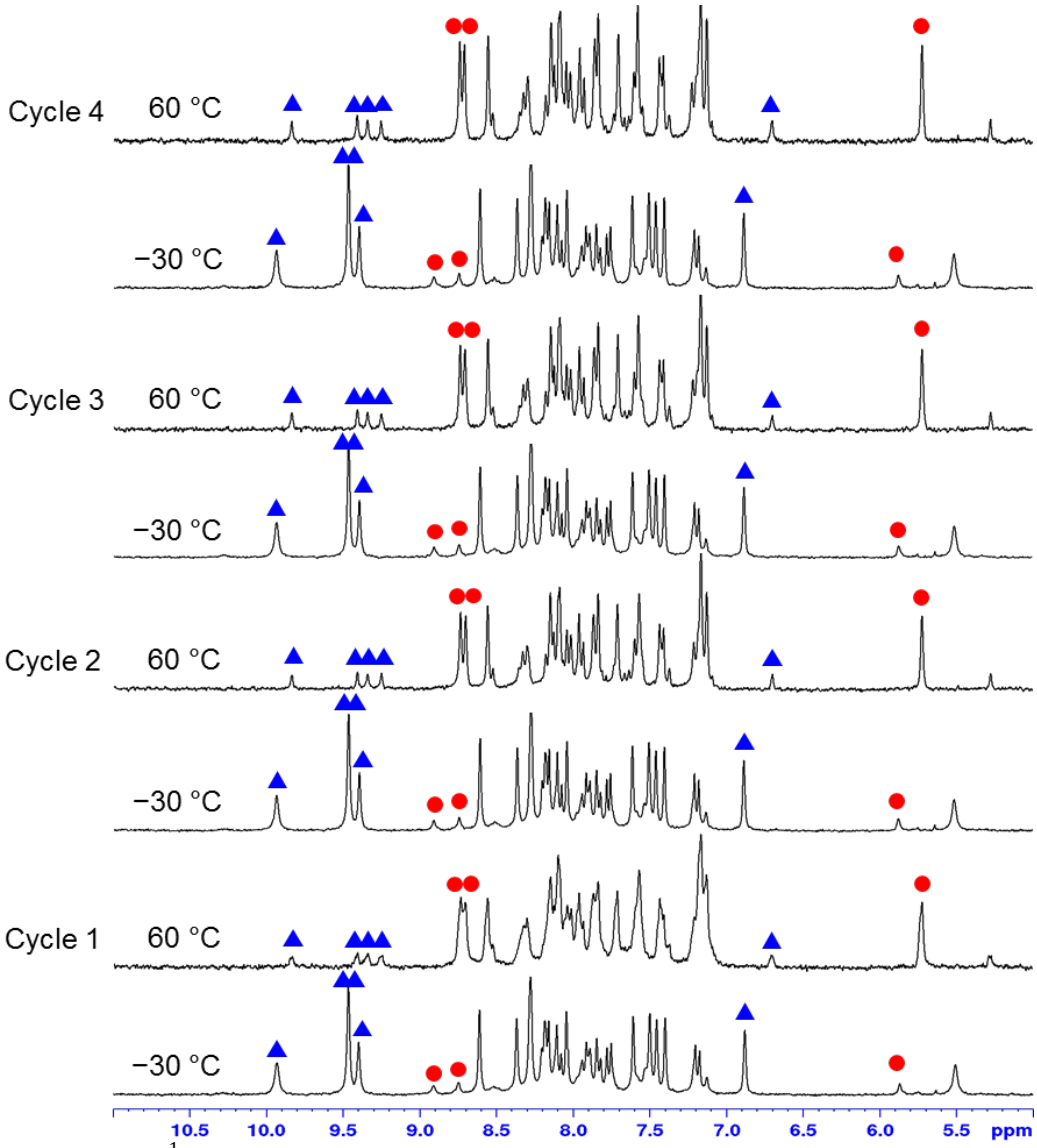

Fig. S10 Partial ^{1}H NMR spectra (300 MHz) of **2** (1.0 mM) in ethyl acetate-d_8 upon cycling temperature from −30 °C to 60 °C. Signals corresponding to **2**(*syn-anti*) and **2**(*syn-syn*) were marked by blue triangles and red circles, respectively.

3. X-ray crystallographic analyses

3.1. Crystal growing

Single crystals of **1** and **2**(*syn-syn*) were obtained by the vapor diffusion of pentane into EtOAc/pentane (1:5, v/v) solutions of **1** and **2**(*syn-syn*), respectively. On the other hand, single crystals of **2**(*syn-anti*) were obtained by slow evaporation of a CH_2Cl_2/hexane (1:1, v/v) solution containing **2**.

3.2 Data collection

The diffraction data were collected at 100 K on an ADSC Quantum 210 CCD diffractometer with synchrotron radiation at Supramolecular Crystallography 2D, Pohang Accelerator Laboratory (PAL), Pohang, Korea. The ADSC Q210 ADX program[S5] was used for data collection (detector distance: 63 mm, omega scan: $\Delta\omega = 1^{o}$, exposure time is 1 sec/frame) and HKL3000sm (Ver. 703r)[S6] was used for cell refinement, reduction and absorption correction.

3.3 Structure solution and refinement

The crystal structures were solved by the direct method with SHELX-XT[S7] and refined by full-matrix least-squares calculations with the SHELX-XL[S8] in the Olex2[S9] program package. The structure solutions of crystals were obtained by the direct methods provided most non-hydrogen atoms from the E-map. The remaining non-hydrogen atoms were located in an alternating series of least-squares cycles and difference Fourier maps. All non-hydrogen atoms were refined with anisotropic displacement coefficients. All hydrogen atoms were included in the structure factor calculation at idealised positions and were allowed to ride on the neighboring atoms with relative isotropic displacement coefficients.

For **1**⊃$2H_2O$, a *t*-butyl group bonded to an indolocarbazole was observed as disordered and modeled using ISOR restraint. The final least-squares refinement of 770 parameters against 13561 data resulted in residuals R (based on F^2 for $I \geq 2\sigma$) and wR (based on F^2 for all data)

[S5] A. J. Arvai and C. Nielsen, *ADSC Quantum-210 ADX Program, Area Detector System Corporation*, Poway, CA, USA, 1983.
[S6] Z. Otwinowski and W. Minor, *Methods in Enzymology*, ed. C. W. Carter Jr. and R. M. Sweet, Academic Press, New York, 1997, Vol. 276, part A, pp. 307–326.
[S7] G. M. Sheldrick, *Acta Cryst.* 2015, ***A71***, 3–8.
[S8] G. M. Sheldrick, *Acta. Cryst*. 2015, ***C71***, 3–8.
[S9] O. V. Dolomanov, L. J. Bourhis, R. J. Gildea, J. A. K. Howard and H. Puschmann, *J. Appl. Cryst.*, 2009, **42**, 339–341.

of 0.0818 and 0.2451, respectively. The final difference Fourier map was featureless.

For the **2**(*syn-anti*), the final least-squares refinement of 774 parameters against 20422 data resulted in residuals R (based on F^2 for $I \geq 2\sigma$) and wR (based on F^2 for all data) of 0.0581 and 0.1753, respectively. The final difference Fourier map was featureless.

For the **2**(*syn-syn*), two different *t*-butyl groups bonded to indolocarbazoles were observed as disordered and modeled using DFIX, SADI, FLAT, RIGU and ISOR restraint. The final least-squares refinement of 3181 parameters against 42189 data resulted in residuals R (based on F^2 for $I \geq 2\sigma$) and wR (based on F^2 for all data) of 0.0925 and 0.2703, respectively. The final difference Fourier map was featureless.

3.4 Summary

1⊃$2H_2O$: Crystal Data for $C_{74}H_{72}N_6O_3$ (*M* =1093.37 g/mol): orthorhombic, space group $P2_12_12_1$ (no. 19), a = 35.034(7) Å, b = 10.393(2) Å, c = 17.979(4) Å, *V* = 6546(2) $Å^3$, *Z* = 4, *T* = 100 K, μ(synchrotron) = 0.066 mm^{-1}, *Dcalc* = 1.109 g/cm^3, 13561 reflections measured (3.198° ≤ 2Θ ≤ 52.998°), 13561 unique (R_{int} = 0.0000, R_{sigma} = 0.0569) which were used in all calculations. The final R1 was 0.0818 ($I > 2\sigma(I)$) and wR2 was 0.2451 (all data).

Table S3. Crystal data and structure refinement for **1**⊃$2H_2O$

Identification code	**1**⊃$2H_2O$
Empirical formula	$C_{74}H_{72}N_6O_3$
Formula weight	1093.37
Temperature/K	100
Crystal system	orthorhombic
Space group	$P2_12_12_1$
a/Å	35.034(7)
b/Å	10.393(2)
c/Å	17.979(4)
α/°	90

β/°	90
γ/°	90
Volume/Å^3	6546(2)
Z	4
Dcalc g/cm^3	1.109
μ/mm^{-1}	0.066
F(000)	2328.0
Crystal size/mm^3	0.45 × 0.315 × 0.22
Radiation	synchrotron (λ = 0.70000)
2Θ range for data collection/°	3.198 to 52.998
Index ranges	-46 ≤ h ≤ 46, -13 ≤ k ≤ 12, -23 ≤ l ≤ 24
Reflections collected	13561
Independent reflections	13561 [R_{int} = 0.0000, R_{sigma} = 0.0569]
Data/restraints/parameters	13561/12/770
Goodness-of-fit on F^2	0.953
Final R indexes [$I > 2\sigma(I)$]	R1 = 0.0818, wR2 = 0.2256
Final R indexes [all data]	R1 = 0.1161, wR2 = 0.2451
Largest diff. peak/hole / e.Å^{-3}	0.85/−0.35

2(*syn-anti*): Crystal Data for $C_{74}H_{68}Cl_2N_6OPd$ (*M* =1234.64 g/mol): monoclinic, space group C2/c (no. 15), a = 31.021(6) Å, b = 22.132(4) Å, c = 29.199(6) Å, β = 119.15(3)°, *V* = 17508(8) Å^3, *Z* = 8, *T* = 100 K, μ(synchrotron) = 0.298 mm^{-1}, *Dcalc* = 0.937 g/cm^3, 39408 reflections measured (3.096° ≤ 2Θ ≤ 56°), 20422 unique (R_{int} = 0.0275, R_{sigma} = 0.0513) which were used in all calculations. The final R1 was 0.0581 ($I > 2\sigma(I)$) and wR2 was 0.1753 (all data).

Table S4. Crystal data and structure refinement for **2**(*syn-anti*)

Identification code	**2**(*syn-anti*)
Empirical formula	$C_{74}H_{68}Cl_2N_6OPd$
Formula weight	1234.64
Temperature/K	100
Crystal system	monoclinic
Space group	C2/c
a/Å	31.021(6)
b/Å	22.132(4)
c/Å	29.199(6)
α/°	90
β/°	119.15(3)
γ/°	90
Volume/Å^3	17508(8)
Z	8
Dcalc g/cm^3	0.937
μ/mm^{-1}	0.298
F(000)	5136.0
Crystal size/mm^3	0.045 × 0.033 × 0.032
Radiation	Synchrotron (λ = 0.70000)
2Θ range for data collection/°	3.096 to 56
Index ranges	-39 ≤ h ≤ 39, -29 ≤ k ≤ 29, -39 ≤ l ≤ 39
Reflections collected	39408
Independent reflections	20422 [R_{int} = 0.0275, R_{sigma} = 0.0513]
Data/restraints/parameters	20422/0/774
Goodness-of-fit on F^2	1.034

Final R indexes [$I > 2\sigma(I)$]	R1 = 0.0581, wR2 = 0.1639
Final R indexes [all data]	R1 = 0.0835, wR2 = 0.1753
Largest diff. peak/hole / e.Å^{-3}	0.54/−1.18

2(*syn-syn*) : Crystal Data for $C_{148}H_{136}Cl_4N_{12}O_2Pd_2$ (M =2469.28 g/mol): triclinic, space group P-1 (no. 2), a = 16.792(2) Å, b = 23.687(2) Å, c = 39.551(3) Å, α = 73.077(2)°, β = 84.189(3)°, γ = 81.240(4)°, V = 14848(2) Å^3, Z = 4, T = 100.0 K, μ(synchrotron) = 0.471 mm^{-1}, *Dcalc* = 1.105 g/cm^3, 82338 reflections measured (2.768° ≤ 2Θ ≤ 52.998°), 42189 unique (R_{int} = 0.1003, R_{sigma} = 0.1322) which were used in all calculations. The final R1 was 0.0925 ($I > 2\sigma(I)$) and wR2 was 0.2703 (all data).

Table S5. Crystal data and structure refinement for **2**(*syn-syn*)

Identification code	**2**(*syn-syn*)
Empirical formula	$C_{148}H_{136}Cl_4N_{12}O_2Pd_2$
Formula weight	2469.28
Temperature/K	100.0
Crystal system	triclinic
Space group	P-1
a/Å	16.792(2)
b/Å	23.687(2)
c/Å	39.551(3)
α/°	73.077(2)
β/°	84.189(3)
γ/°	81.240(4)
Volume/Å^3	14848(2)
Z	4

Dcalc g/cm^3	1.105
μ/mm^{-1}	0.471
F(000)	5136.0
Crystal size/mm^3	0.02 × 0.005 × 0.005
Radiation	Synchrotron (λ = 0.80000)
2Θ range for data collection/°	2.768 to 52.998
Index ranges	-18 ≤ h ≤ 18, -26 ≤ k ≤ 26, -44 ≤ l ≤ 44
Reflections collected	82338
Independent reflections	42189 [R_{int} = 0.1003, R_{sigma} = 0.1322]
Data/restraints/parameters	42189/291/3181
Goodness-of-fit on F^2	1.052
Final R indexes [$I > 2\sigma(I)$]	R1 = 0.0925, wR2 = 0.2418
Final R indexes [all data]	R1 = 0.1448, wR2 = 0.2703
Largest diff. peak/hole / e.Å^{-3}	1.33/−1.63

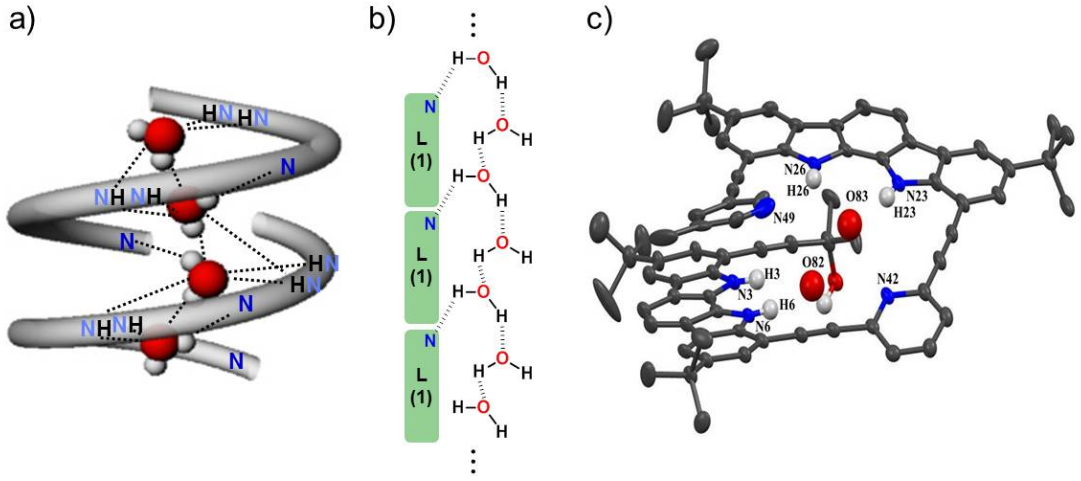

Fig. S11 (a), (b) Schematic representation of the hydrogen bonding network observed in the crystal structure of **1**⊃2H_2O, and (c) thermal ellipsoid representation of **1**⊃2H_2O.

Table S6. Hydrogen-bonding distances (Å) in the crystal structure of **1**⊃2H_2O.

Donor···Acceptor	Distance
O(82)···N(49)	2.983
O(82) ···O(83)	3.185
N(23) ···O(83)	2.991
O(83) ···N(42)	2.804
N(3) ···O(82)	3.165
N(6) ···O(82)	3.033

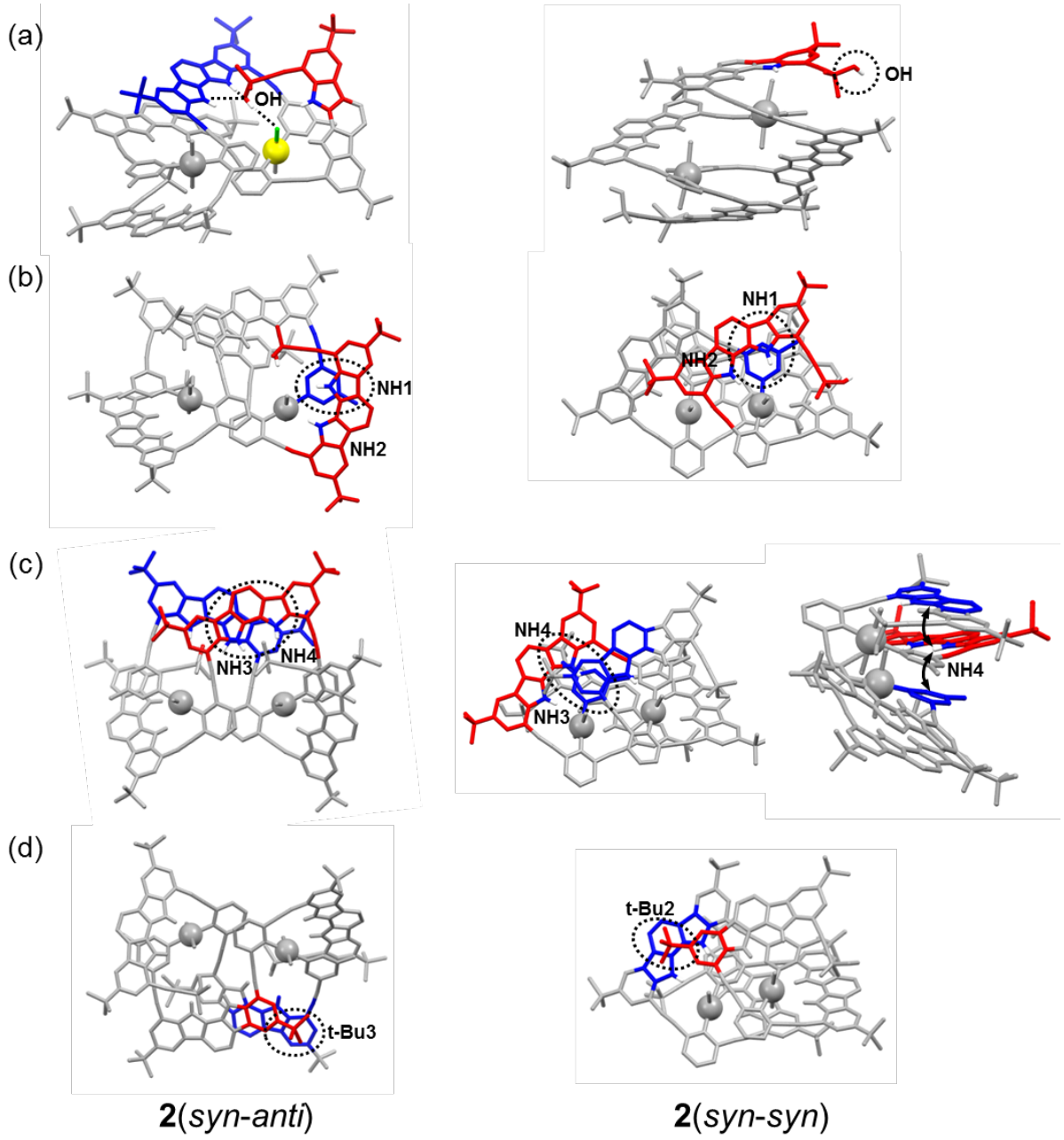

Fig. S12 Several different views of the X-ray crystal structures of **2**(*syn-anti*) and **2**(*syn-syn*).

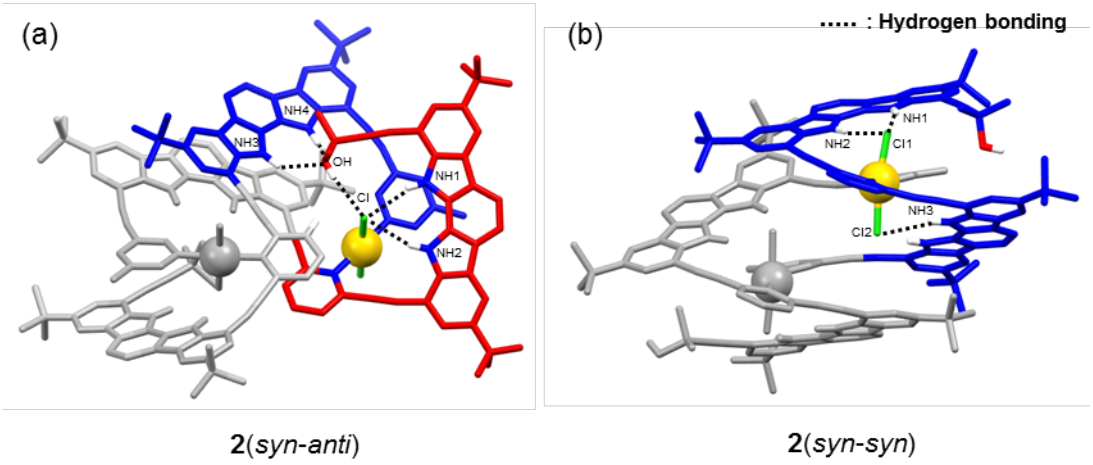

Fig. S13 Hydrogen-bonding networks observed in the crystal structures of (a) **2**(*syn-anti*) and (b) **2**(*syn-syn*).

Table S7. Hydrogen-bonding distances (Å) and angle (°) in the crystal structure of **2**(*syn-anti*) and **2**(*syn-syn*).

	Donor···Acceptor	Distance	Angle (DHA)
2(*syn-anti*)	NH1···Cl	2.565	158.14
	NH2···Cl	2.563	158.96
	OH···Cl	2.586	166.33
	NH3···O	2.273	137.76
	NH4···O	2.307	139.12
2(*syn-syn*)	NH1···Cl1	2.528	156.07
	NH2···Cl1	2.360	163.14
	NH3···Cl2	2.556	165.36

4. ESI-MS Spectra

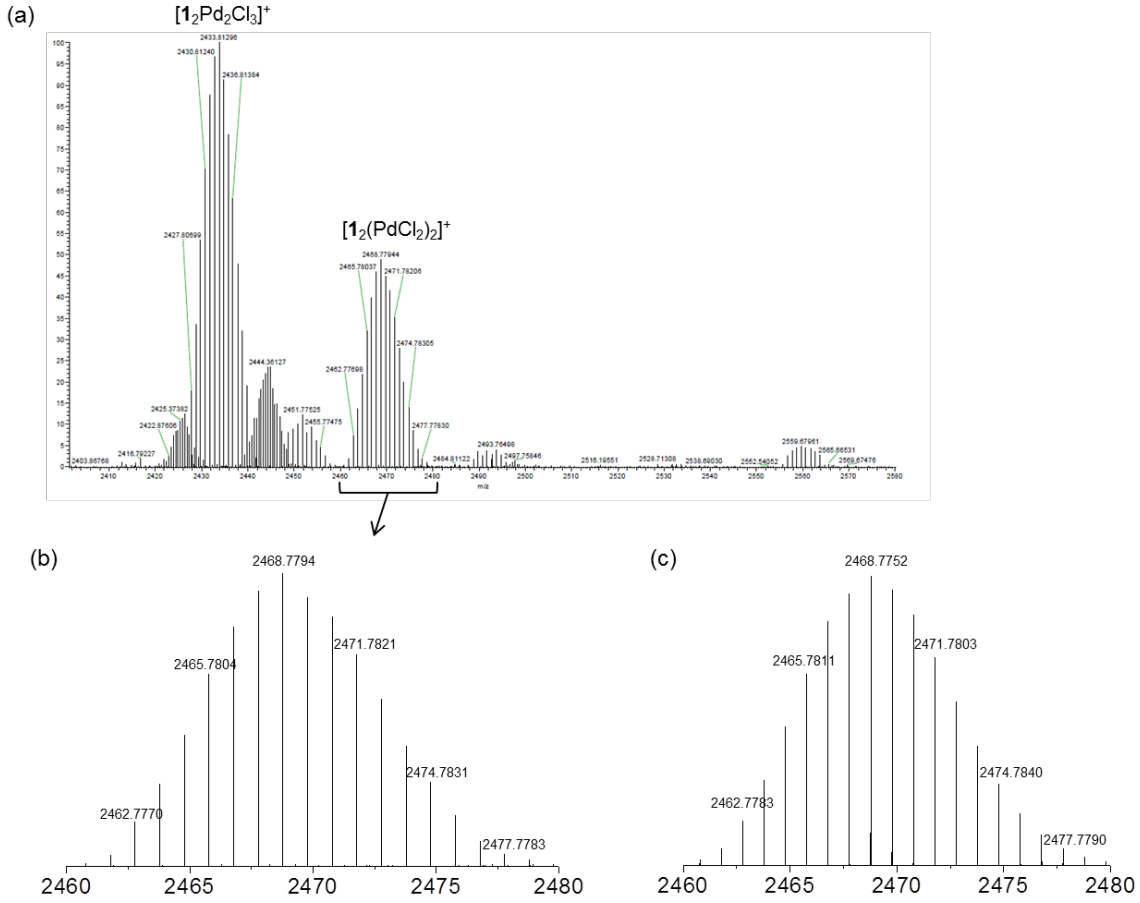

Fig. S14 (a) High resolution ESI-MS data of helicate **2**, and (b) experimental and (c) theoretical isotopic distributions for $[\mathbf{1}_2(PdCl_2)_2]^+$ (m/z = 2469).

5. NMR Spectra

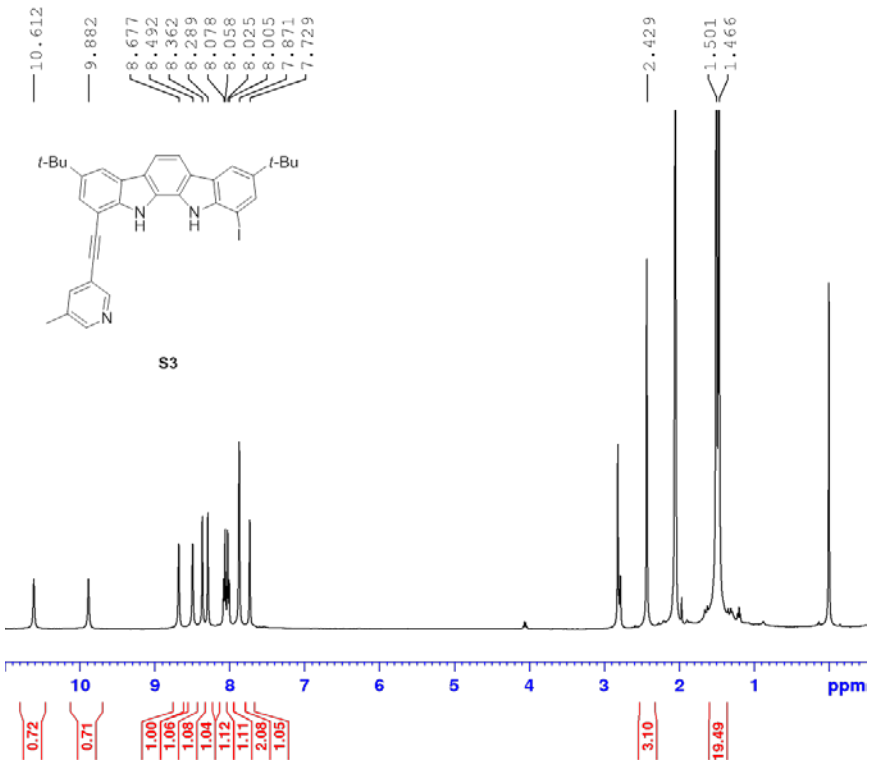

Fig. S15 ^{1}H NMR of **S3** (400 MHz, acetone-d_6, 25 °C)

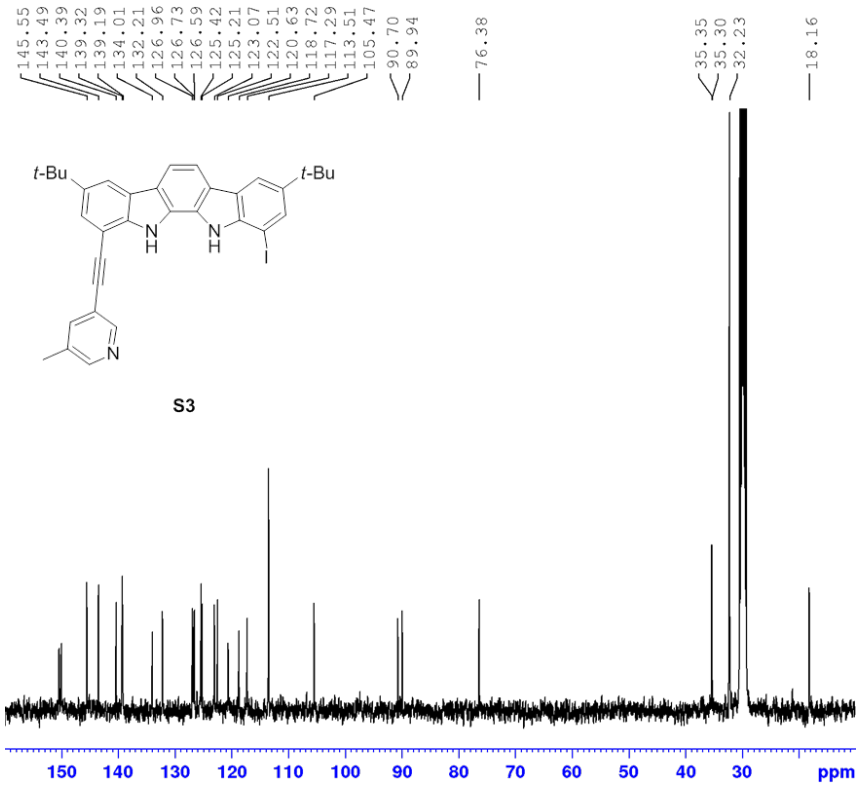

Fig. S16 ^{13}C NMR of **S3** (100 MHz, acetone-d_6, 25 °C)

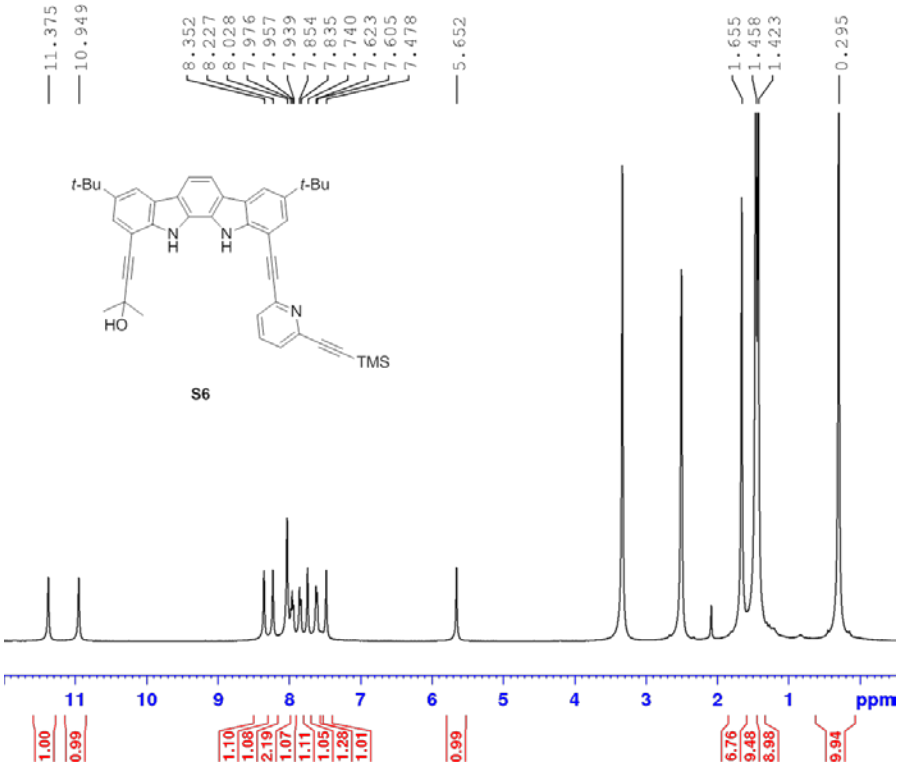

Fig. S17 ^{1}H NMR of **S6** (400 MHz, DMSO-d_6, 25 °C)

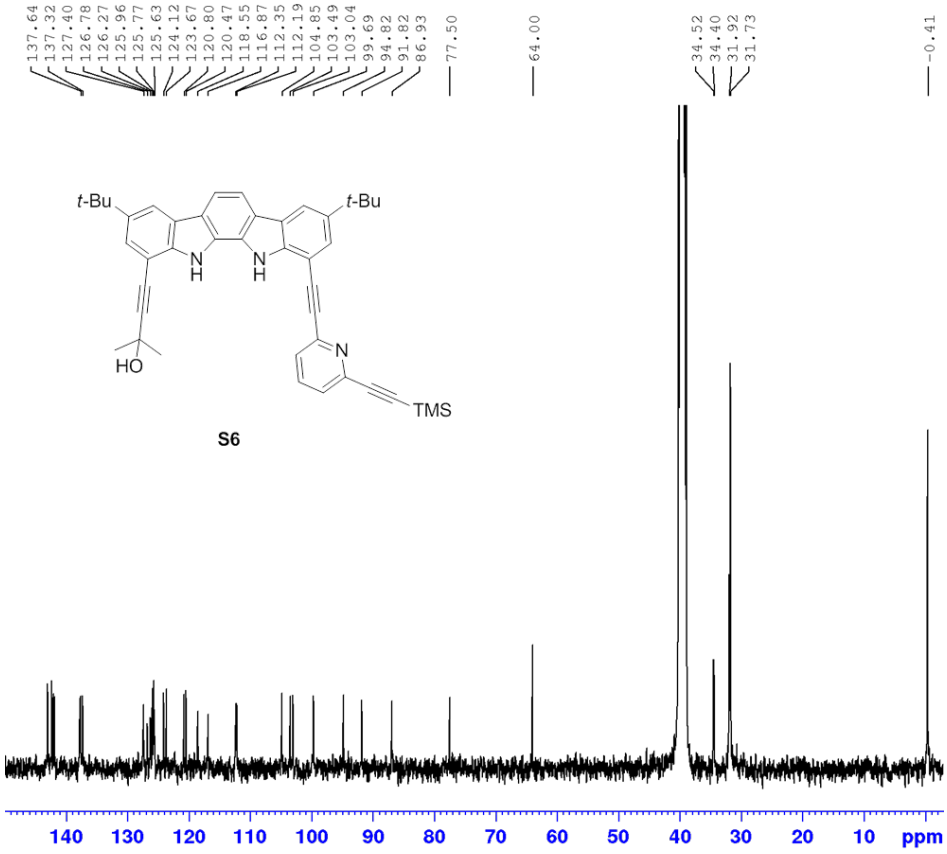

Fig. S18 ^{13}C NMR of **S6** (100 MHz, DMSO-d_6, 25 °C)

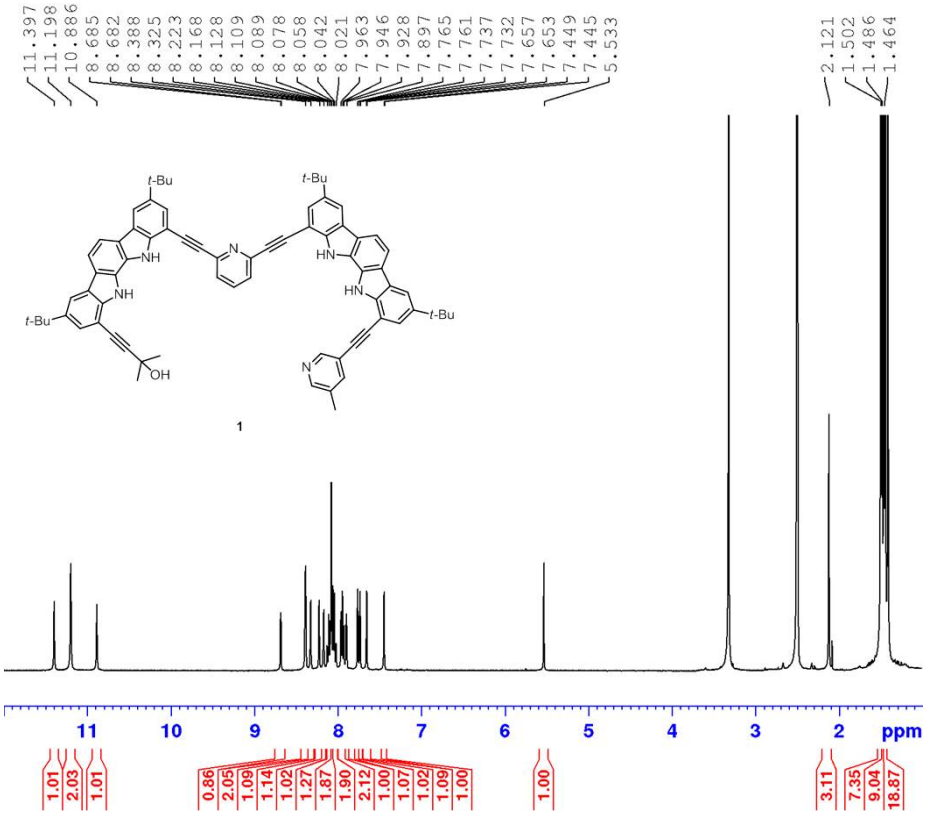

Fig. S19 ^{1}H NMR of **1** (400 MHz, DMSO-d_6, 25 °C)

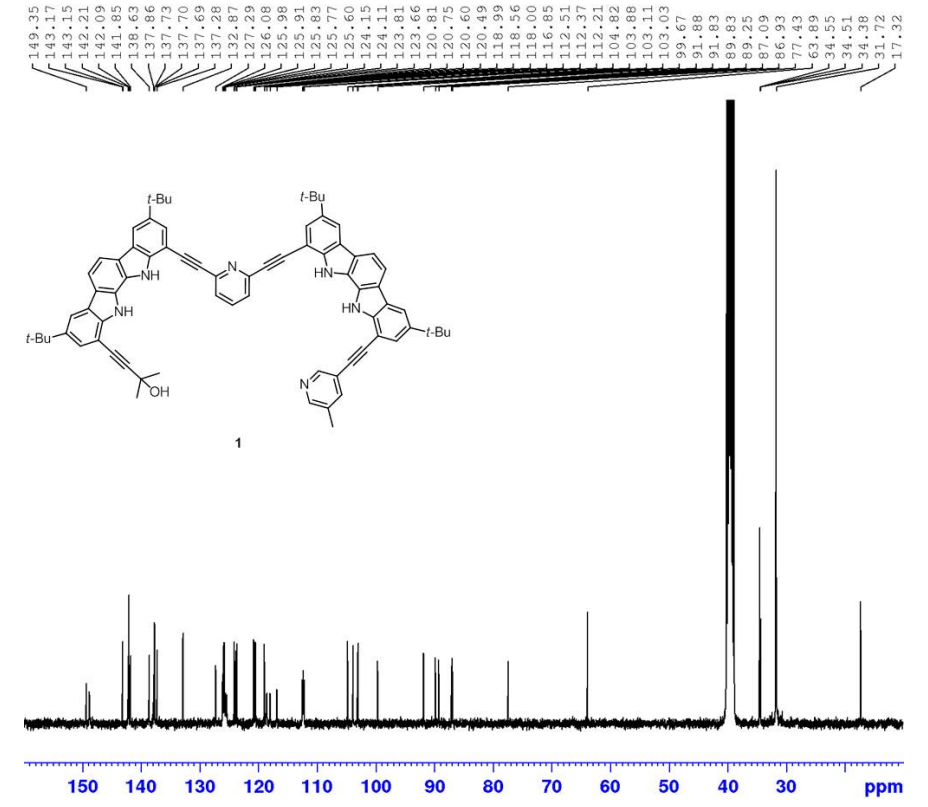

Fig. S20 ^{13}C NMR of **1** (100 MHz, DMSO-d_6, 25 °C)

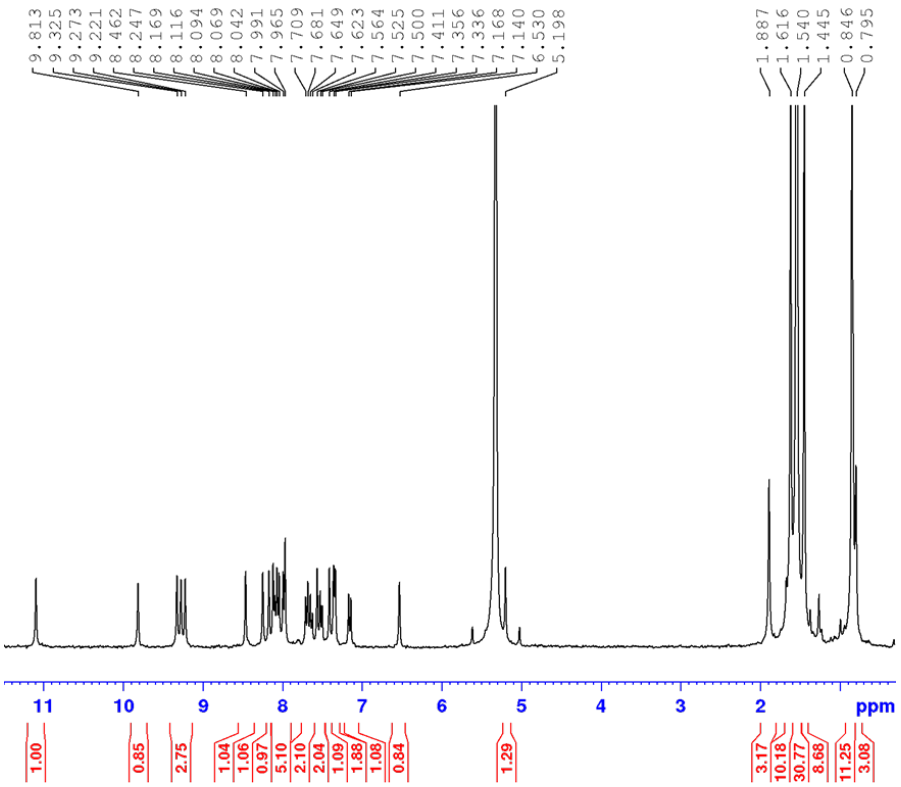

Fig. S21 ^{1}H NMR of **2** (400 MHz, CD_2Cl_2, 25 °C)

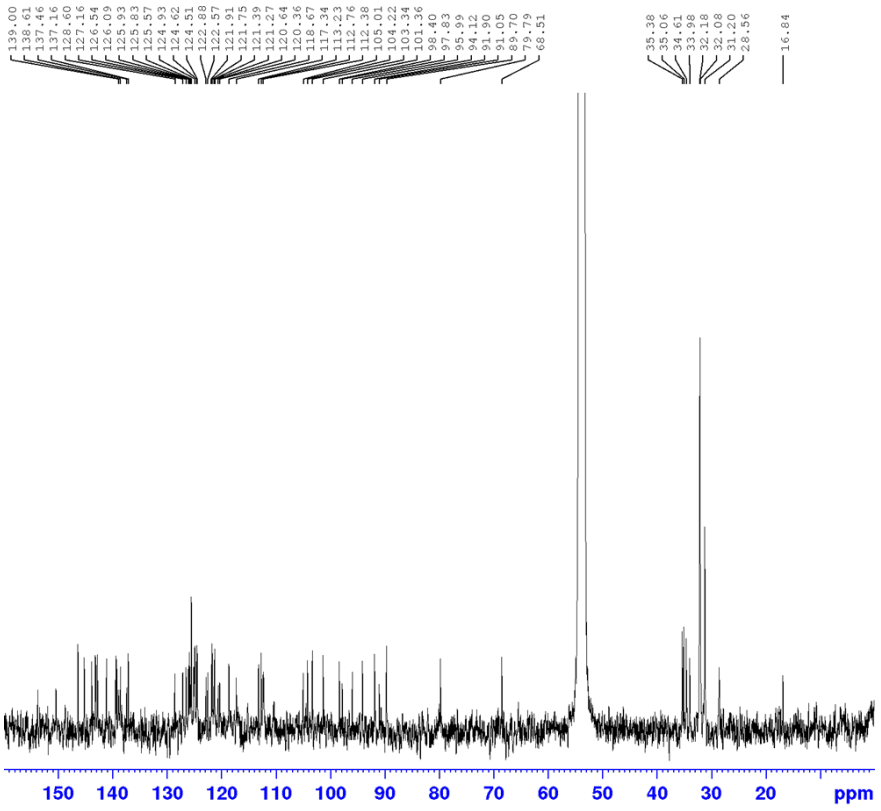

Fig. S22 ^{13}C NMR of **2** (100 MHz, CD_2Cl_2, 25 °C)